Clin. Lab. 2026;72:XXX-XXX

ORIGINAL ARTICLE

A Peripheral Blood Circular Ribonucleic Acid-Based Nomogram for Risk Stratification in Chronic Myeloid Leukemia

Yuanyuan Bai [1], Xiangjun Li [1, 2], Yingying Wang [1], Zhanguo Chen [1]

[1] *Department of Clinical Laboratory, The Second Affiliated Hospital and Yuying Children's Hospital of Wenzhou Medical University, Wenzhou, Zhejiang, China*
[2] *Scientific Research Center, Wenzhou Medical University, Wenzhou, Zhejiang, China*

ABSTRACT

Background: **Current prognostic tools for chronic myeloid leukemia (CML) rely primarily on clinical parameters and lack reliable molecular biomarkers for dynamic risk assessment. Circular RNAs (circRNAs) have emerged as promising liquid biopsy biomarkers because of their stability in peripheral blood. However, their prognostic value in CML remains underexplored.**
Methods: **In this retrospective cohort study, peripheral blood samples were collected from 417 patients newly diagnosed with CML and 45 healthy controls. Differentially expressed circRNAs were identified by high-throughput sequencing and validated by quantitative real-time PCR. The patients were randomly divided into training (n = 292) and validation (n = 125) cohorts. A prognostic nomogram incorporating circRNAs and clinical variables was developed using multivariate Cox regression, with model performance assessed using the area under the curve (AUC), calibration, and decision curve analysis.**
Results: **Two circRNAs (hsa_circ_0001523 and hsa_circ_0000095) were significantly dysregulated in patients with advanced-phase CML ($p < 0.0001$). The nomogram combining the expression patterns of two circRNAs with basophil%, blast%, and hemoglobin levels achieved an AUC of 0.920 (95% CI: 0.873 - 0.968) for survival prediction. High-risk patients (score > 122.5) had a significantly shorter median survival (22 vs. 83 months, $p < 0.0001$).**
Conclusions: **This circRNA-based nomogram is a clinically applicable, non-invasive tool for dynamic risk stratification in CML. The integration of molecular and hematological markers may guide personalized therapy decisions and address the limitations of existing prognostic systems.**
(Clin. Lab. 2026;72:xx-xx. DOI: 10.7754/Clin.Lab.2025.251027)

Correspondence:
Zhanguo Chen
Department of Clinical Laboratory
The Second Affiliated Hospital and
Yuying Children's Hospital of
Wenzhou Medical University
1111 Wenzhou Avenue
Longwan District, Wenzhou
Zhejiang, 325024
China
Phone: +86 13634250633
Email: steve0577@126.com

Manuscript accepted November 20, 2025

KEYWORDS

chronic myeloid leukemia, circRNA, nomogram, prognosis, peripheral blood biomarker

INTRODUCTION

Chronic myeloid leukemia (CML), a clonal hematopoietic malignancy, has an annual incidence of 1.6 - 2 cases per 100,000 individuals worldwide [1,2]. Tyrosine kinase inhibitors (TKIs) have achieved 10-year survival rates > 80% [3]. However, 20 - 30% of patients experience treatment failure, predominantly due to drug resistance or blast crisis progression [4,5]. Current prognostic tools (e.g., Sokal, Hasford, and EUTOS scores) rely solely on clinical parameters such as spleen size and

blast counts [6,7]. In addition, they lack dynamic molecular biomarkers for real-time risk assessment. This limitation underscores the urgent need for noninvasive serial monitoring tools to guide personalized therapy decisions.

Circular RNAs (circRNAs) have gained considerable attention as stable and liquid biopsy-compatible biomarkers, owing to their covalently closed structures and resistance to degradation [8,9]. Dysregulated circRNAs that modulate key oncogenic pathways in CML, such as hsa_circ_0006010 and hsa_circ_0002903, are potential diagnostic markers [10]. Another potential diagnostic marker is circBA9.3, which enhances TKI resistance by upregulating BCR-ABL1 expression [11]. Additionally, Circ_0009910 promotes imatinib resistance in CML by modulating ULK1-induced autophagy through miR-34a-5p targeting [12]. Despite these advances, critical gaps remain in the literature. Although exosomal circRNAs (e.g., circ_0006896) have been clinically validated as prognostic biomarkers of acute myeloid leukemia (AML) [13], no validated peripheral blood circRNA-based prognostic model exists for CML.

Nomograms can integrate continuous variables and provide individualized risk quantification [14]. Consequently, they have become indispensable prognostic tools in oncology, particularly for hematologic malignancies. Existing nomograms for CML primarily rely on hematological and cytogenetic markers [7]. However, none have leveraged the emerging potential of circRNAs recently implicated in CML. Our preliminary studies identified hsa_circ_0001523 and hsa_circ_0000095 as phase-specific markers of CML (GEO accession: GSE212254). We hypothesized that peripheral blood circRNAs (hsa_circ_0001523 and hsa_circ_0000095) could serve as stable, non-invasive biomarkers for CML prognosis, thereby complementing existing clinical parameters. To test this hypothesis, we first identified phase-specific circRNAs in CML progression through high-throughput sequencing and subsequently developed the first circRNA-based nomogram that integrated these molecular markers with hematologic parameters for survival prediction. Finally, we rigorously validated the clinical utility of the model for risk stratification and therapeutic guidance. This study addresses a critical, unmet need by bridging molecular insights with clinical practicality, potentially transforming CML management through liquid biopsy-based prognostication.

MATERIALS AND METHODS

Study profile

A total of 477 newly diagnosed CML patients were screened for eligibility between January 2015 and December 2020 at the Second Affiliated Hospital and Yuying Children's Hospital of Wenzhou Medical University. After excluding patients with missing key clinical or survival data (n = 39), history of or concurrent non-CML malignancy (n = 17), or follow-up duration < 6 months (n = 4), 417 patients were included in the final analysis. Meanwhile, 45 healthy individuals from the physical examination center of the hospital were recruited as the healthy controls. Diagnosis and disease staging were performed according to the European LeukemiaNet (ELN) 2013 criteria for CML [15]. Response to treatment is defined in the ELN recommendations [16]. Patients were randomly assigned to the training (n = 292) or validation (n = 125) cohorts using a stratified randomization method based on the CML phase to ensure a balanced phase distribution between the groups. The training set comprised 50 and 242 patients with advanced- and chronic-phase CML, respectively. In contrast, the validation set included 28 and 97 patients with advanced- and chronic-phase CML, respectively. The collected clinical data for complete blood count parameters included the white blood cell (WBC) count, neutrophil%, basophil%, eosinophil%, blast%, hemoglobin levels, red blood cell (RBC) count, RDW-CV, and platelet count. The characteristics of patients with CML in the training and validation sets are presented in Supplementary Table S1. Written informed consent was obtained from all the participants, and the study protocol was approved by the Ethics Committee of the Second Affiliated Hospital and Yuying Children's Hospital of Wenzhou Medical University.

Sample collection

Peripheral blood samples (2 mL) were collected in EDTA-K2 tubes for RNA extraction. Peripheral blood mononuclear cells were first prepared through Ficoll Hypaque gradient centrifugation, and then immediately lysed in 1 mL of TRIzol® reagent (Invitrogen, USA) and maintained at -70°C until further processing.

Experimental detection and data analysis for key circRNAs

Identification of key circRNAs

Differentially expressed circRNAs were identified in peripheral blood samples from three patients with chronic-phase CML, three with advanced-phase CML, and three healthy controls using high-throughput sequencing (Novogene, Beijing). CircRNAs with $|\log2(\text{fold change})| \geq 2.0$ and adjusted p-value < 0.05 (Benjamini-Hochberg correction for multiple testing) were considered significant [17]. All identified circRNAs were cross-referenced using circBase [18] to exclude sequencing artifacts. A set of significantly differentially expressed circRNAs was detected, including candidates with upregulated and downregulated expression (GSE212254). Among these, hsa_circ_0001523 and hsa_circ_0000095 were identified as key circRNAs of interest. The experimental primers were designed and provided by RIBOBIO, and the sequences are listed in Supplementary Table S2.

RNA reverse transcription and quantitative real-time PCR (qRT-PCR) validation

Following extraction, total RNA was recovered in 50 μL of RNase free water. Its concentration and quality were subsequently assessed using a NanoDrop ND-1000 spectrophotometer (Thermo Fisher Scientific, USA). Total RNA was reverse-transcribed using the PrimeScript™ RT reagent kit (Takara, Japan) for cDNA synthesis. qRT-PCR was performed using TB Green Premix Ex Taq II (Takara, Japan) on an ABI 7500 system (Applied Biosystems) under standardized conditions. The relative expression levels of hsa_circ_0001523 and hsa_circ_0000095 were calculated using the $2^{(-\Delta\Delta Ct)}$ method [19], with GAPDH as the reference gene. Primer specificity was confirmed by a single melting curve peak using qRT-PCR. All reactions were performed in triplicate using three independent biological samples.

Identification of prognostic factors via cox regression analysis

The cohort was randomly stratified into the training and independent validation sets. Intergroup comparability was verified using Fisher's exact and Wilcoxon rank-sum tests for categorical and continuous variables, respectively. A training cohort was used to evaluate the association between clinical variables and overall survival (OS). Variables demonstrating statistical significance ($p < 0.05$) in the univariate analysis were subsequently entered into a multivariate Cox regression model to identify independent prognostic factors. The analysis yielded hazard ratios (HR) with 95% confidence intervals and the corresponding regression coefficients for each significant covariate.

Development and validation of the prognostic nomogram

The nomogram model was constructed with the training set using the rms package in R software; the independent prognostic factors identified in the multivariate analysis were incorporated. Scoring standards were established based on the regression coefficients of each factor, and individual scores were assigned accordingly. The total score for each patient was derived by summing these values, which were then converted into the predicted probabilities of 1-year, 3-year, and 5-year OS using a predefined function. To evaluate model performance, receiver operating characteristic (ROC) curves were generated for both the training and validation sets using the survival ROC package; the area under the curve (AUC) served as a measure of discriminative analysis (DCA). Calibration plots were used to compare the predicted probabilities with the observed survival probabilities and assess the accuracy of the model. The median total score was used as the cutoff value to stratify the patients into high- and low-risk groups. A survival analysis was performed to evaluate the prognostic capability of the model for these subgroups.

Statistical analysis

Statistical analyses were conducted using SPSS 24.0 and R 4.2.2. Continuous variables are expressed as the mean ± standard deviation or median (interquartile range) and compared using Student's *t*-test. Categorical variables are presented as counts and percentages and were analyzed using the chi-squared test. Univariate and multivariate Cox regression analyses were performed to identify statistically significant variables for inclusion in the nomograms. Survival analysis was conducted using Kaplan-Meier curves, and differences in survival rates were assessed using the log-rank test. The primary outcome was overall survival (OS), defined as the time from confirmed CML diagnosis to death from any cause. The secondary outcome was progression-free survival (PFS), defined as the time from diagnosis to disease progression (accelerated phase or blast crisis) or death, whichever occurred first. Statistical significance was defined as a two-sided p-value < 0.05.

RESULTS

qRT-PCR detection of key circRNAs in CML progression

qRT-PCR was performed to measure the relative expression levels of key circRNAs in patients in the advanced and chronic phases, and in healthy controls. Significant differences were observed in hsa_circ_0001523 expression between the advanced and chronic phases ($p < 0.0001$) and between the advanced phase and healthy controls ($p < 0.0001$), but not between the chronic phase and healthy controls ($p > 0.05$) (Figure 1A). Similarly, hsa_circ_0000095 expression was significantly dysregulated in patients with advanced-phase CML compared to that in both patients with chronic-phase CML and healthy controls ($p < 0.0001$), whereas no significant difference was observed between patients with chronic-phase CML and healthy controls ($p > 0.05$) (Figure 1B). Furthermore, hsa_circ_0001523 expression was significantly upregulated ($p < 0.0001$) in patients with advanced-phase CML (accelerated phase/blast crisis), whereas that of hsa_circ_0000095 was markedly downregulated ($p < 0.0001$).

ROC curves of key circRNAs in CML progression

ROC curves were constructed for hsa_circ_0001523 and hsa_circ_0000095 expression levels to explore the association between key circRNAs and CML progression. The diagnostic performance of hsa_circ_0001523 yielded an AUC of 0.749 (95% CI: 0.664 - 0.834), with 82.61% specificity and 60.00% sensitivity (Figure 2A). The AUC for hsa_circ_0000095 was 0.779 (95% CI: 0.686 - 0.872), with a specificity of 79.17% and a sensitivity of 67.35% (Figure 2B). These results suggest that the relative expression levels of hsa_circ_0001523 and hsa_circ_0000095 have moderate predictive efficacy for CML progression.

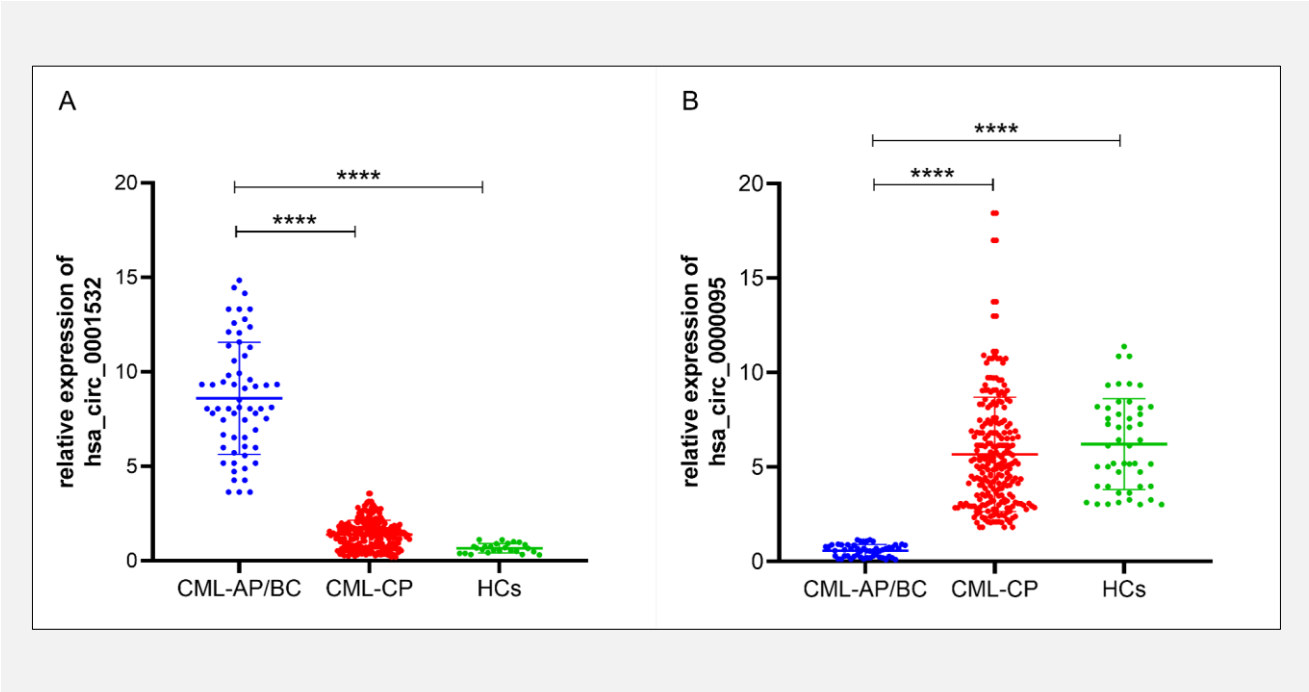

Figure 1. Scatter plots of key circRNA expression levels in CML groups and healthy controls.

Relative expression of hsa_circ_0001523 (A) and hsa_circ_0000095 (B) across groups. ** $p < 0.001$, *** $p < 0.0001$.

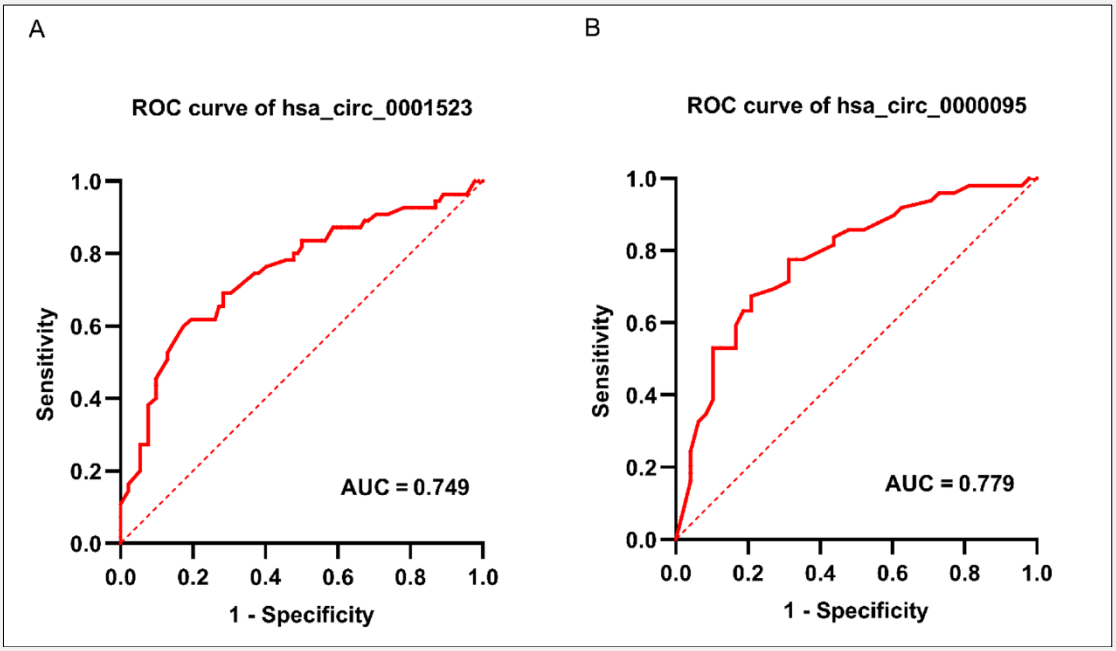

Figure 2. ROC curves for (A) hsa_circ_0001523 and (B) hsa_circ_0000095 in patients with advanced-phase CML.

AUC = 0.749 and 0.779, respectively.

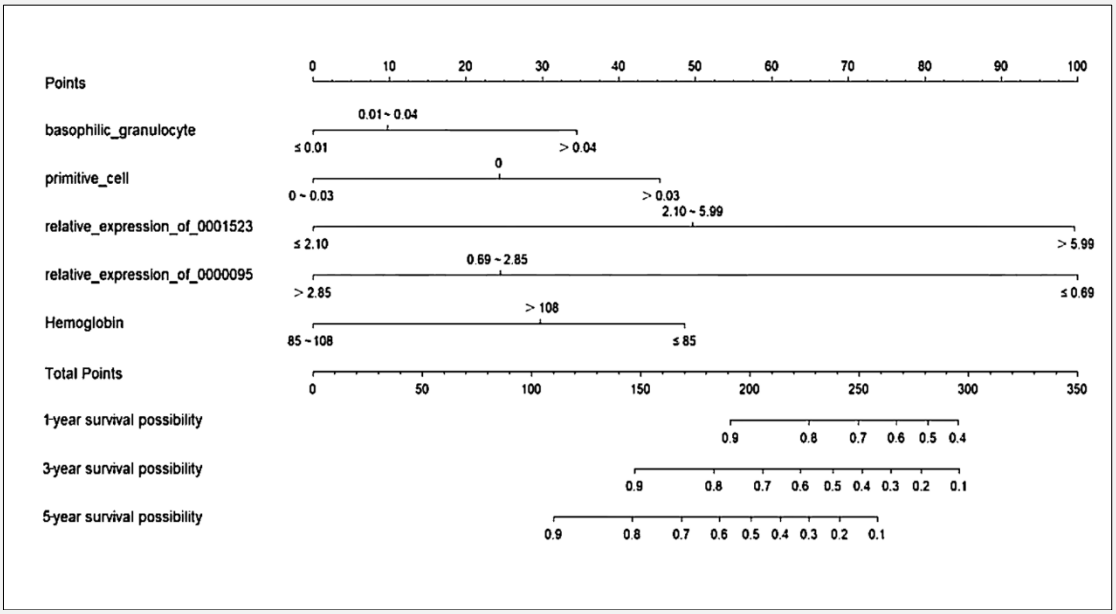

Figure 3. The nomogram for predicting 1-, 3-, and 5-year overall survival in patients with CML.

The nomogram integrates hsa_circ_0001523, hsa_circ_0000095, basophil%, blast%, and hemoglobin data. Each variable corresponds to a point scale. Total points are converted to predicted survival probabilities.

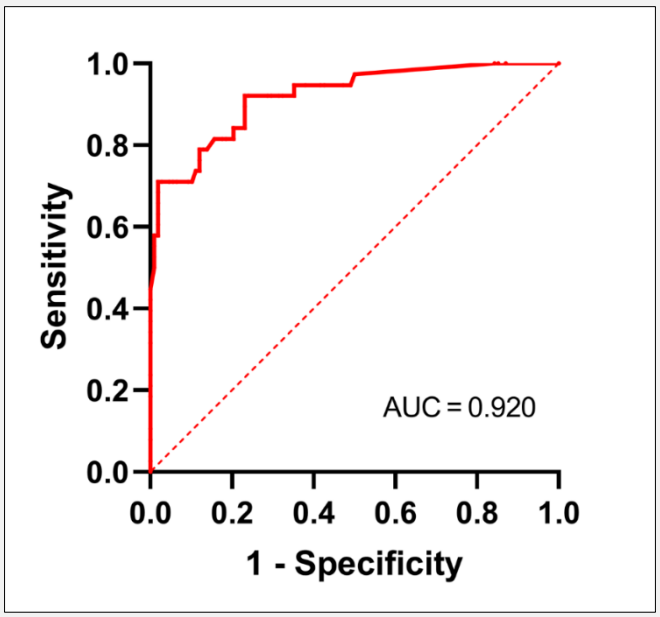

Figure 4. The ROC curve of the nomogram.

AUC = 0.920 (95% CI: 0.873 - 0.968).

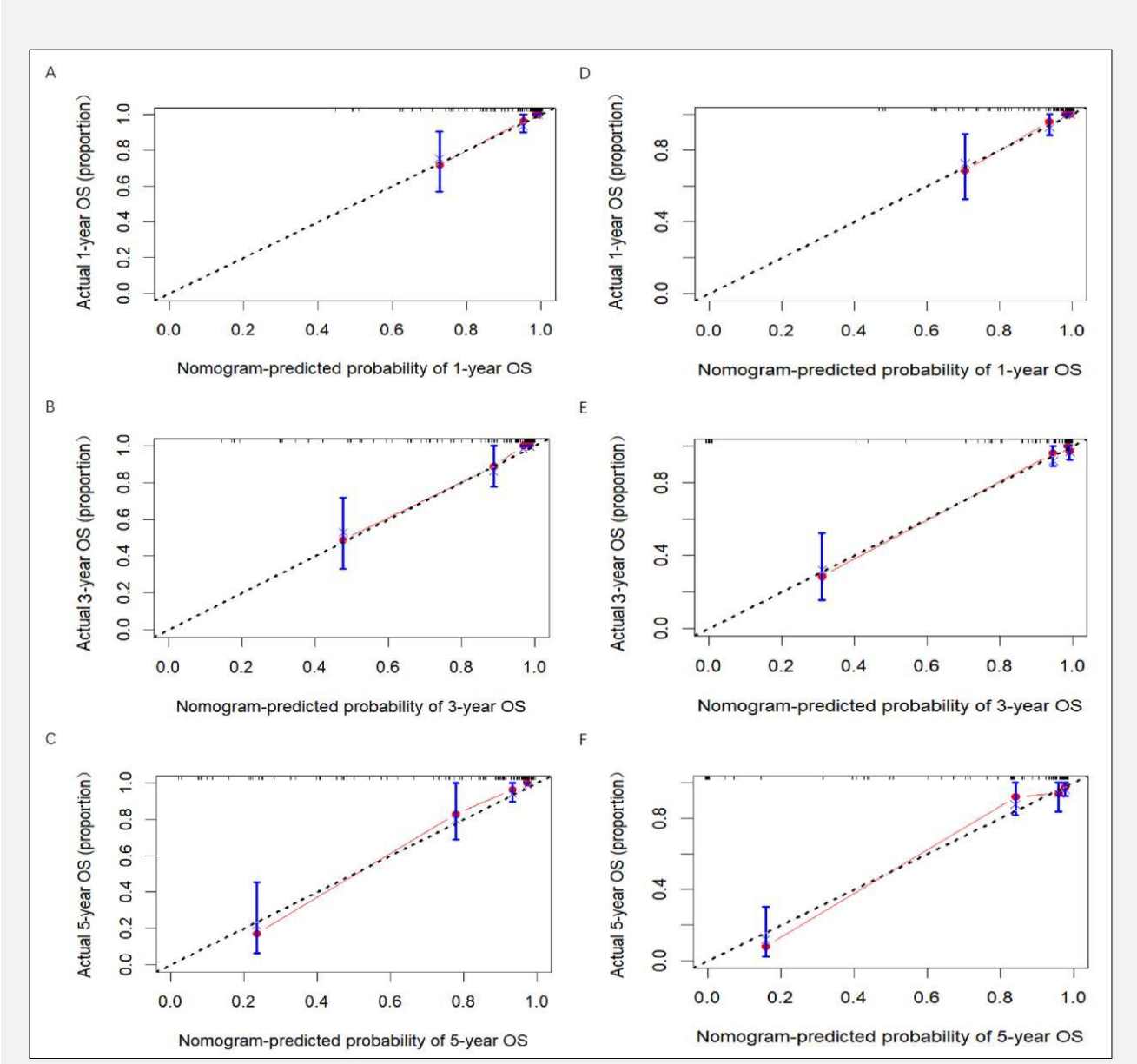

Figure 5. Calibration curves for 1-, 3-, and 5-year survival in the (A - C) training and (D - F) validation sets.

The x- and y-axes represent predicted and observed survival probability, respectively. The diagonal dashed line indicates perfect calibration.

Identification of prognostic factors

Univariate Cox regression analysis (Supplementary Table S3) revealed that age, relative expression levels of hsa_circ_0001523 and hsa_circ_0000095, CML phase, WBC count, basophil%, eosinophil%, blast%, hemoglobin levels, platelet count, and splenomegaly status were significantly associated with overall survival ($p < 0.05$). Multivariate Cox regression analysis identified hsa_circ_0001523, hsa_circ_0000095, basophil%, blast%, and hemoglobin levels as independent prognostic factors for overall survival ($p < 0.05$); these were subsequently included in the nomogram model. These findings underscore the combined prognostic value of molecular and hematological markers in patients with CML.

Construction and validation of the prognostic nomogram model

A nomogram was constructed using R software based on the relative expression levels of hsa_circ_0001523

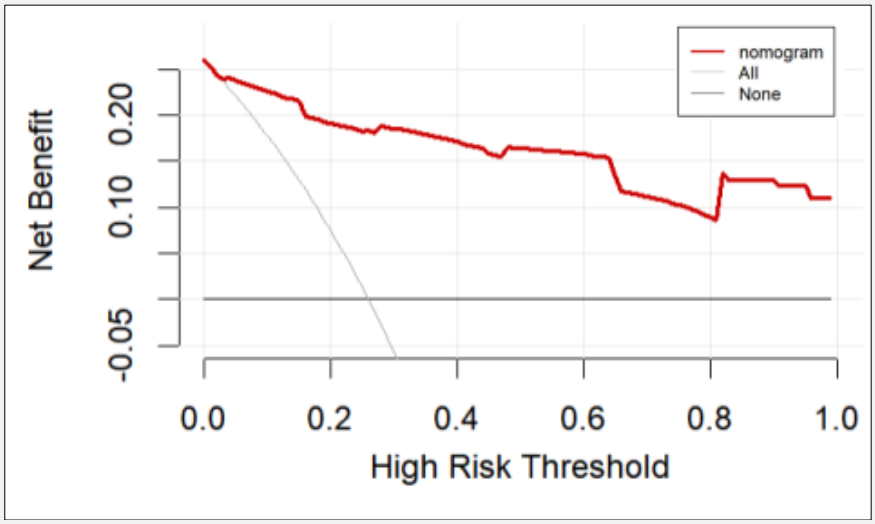

Figure 6. DCA of the nomogram.

The x- and y-axes represent the threshold probability and net benefit rate, respectively. Net benefit was calculated as the difference between the proportions of true and false positives weighted by the threshold probability.

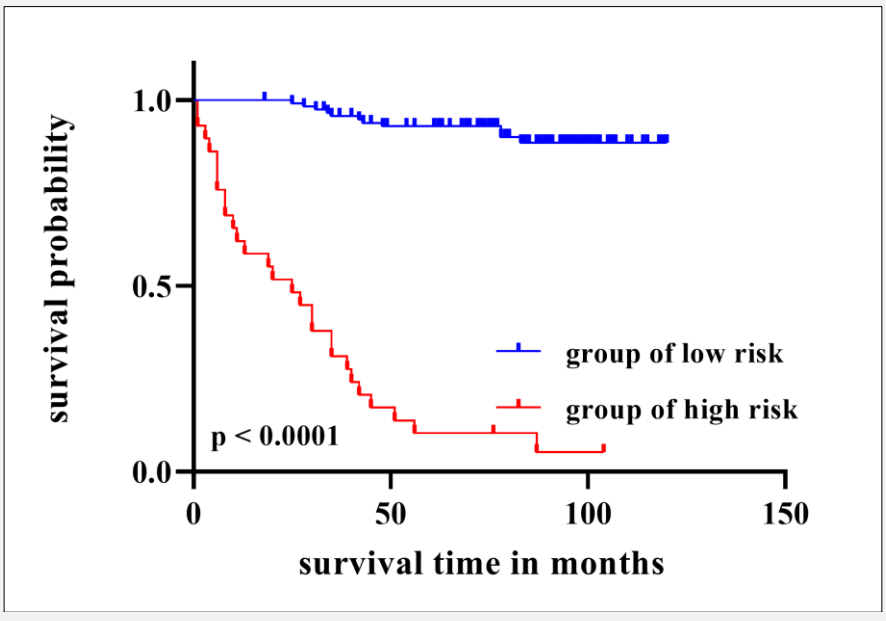

Figure 7. Kaplan-Meier survival curves for high- and low-risk patients with CML.

and hsa_circ_0000095, basophil%, blast%, and hemoglobin levels (Figure 3). The ROC curve of the nomogram had an AUC of 0.920 (95% CI: 0.873 - 0.968) (Figure 4), which was higher than that of single variables, confirming its superior predictive efficacy.

Calibration curves were used to assess the agreement between predicted and observed probabilities. The results showed good agreement between the predicted and actual probabilities for 1-, 3-, and 5-year survival in both the training and validation sets (Figure 5), indicating the high accuracy of the nomogram. DCA revealed that the nomogram provided significant net benefit across a threshold probability range of 0.03 - 1.0, demonstrating its clinical utility (Figure 6).

Survival analysis of patients with CML

Kaplan-Meier survival curves for different prognostic factors

Kaplan-Meier survival curves were plotted for the training set, and differences in survival rates were compared using the log-rank test (Supplementary Figure 1). Significant differences in survival were observed for hsa_circ_0001523, hsa_circ_0000095, age, WBC count, neutrophil%, basophil%, blast%, hemoglobin levels, RBC count, RDW-CV, platelet count, and splenomegaly ($p < 0.05$).

Kaplan-Meier survival curves for high- and low-risk groups

The optimal cutoff value of the nomogram score was determined by maximizing Youden's index (sensitivity + specificity - 1) on the ROC curve of the training set, yielding a cutoff of 122.5. Based on the optimal cutoff value, all patients were stratified into two groups: those with a nomogram score ≤ 122.5 were classified as low-risk (n = 364), whereas patients with a score > 122.5 were classified as high-risk (n = 53). The high-risk group had a median survival time of 22 months compared with 83 months in the low-risk group. The Kaplan-Meier survival curves showed a significant difference between the two groups ($p < 0.0001$), with high-risk patients experiencing a higher probability of adverse events (Figure 7).

DISCUSSION

Recent studies have elucidated the regulatory roles of circRNAs in CML pathogenesis, particularly their contribution to disease progression and treatment resistance. The structural stability and tissue-specific expression patterns of circRNAs make them promising biomarkers that may refine the diagnosis and prognosis of CML. The present study demonstrated the distinct expression patterns of hsa_circ_0001523 and hsa_circ_0000095 during CML progression. The marked upregulation of hsa_circ_0001523 expression and concurrent downregulation of hsa_circ_0000095 expression in patients with advanced-phase CML implicate these circ RNAs in CML progression. These results align with those of previous studies demonstrating circRNA dysregulation in leukemia, wherein circRNAs act as miRNA sponges or protein decoys to regulate critical oncogenic pathways [20,21]. ROC curve analysis further substantiated the diagnostic utility of hsa_circ_0001523 and hsa_circ_0000095, with AUC values of 0.749 and 0.779, respectively. This suggests their potential as standalone prognostic markers. The combined use of these circRNAs may enhance diagnostic precision, thereby addressing the limitations of traditional biomarkers in CML risk stratification [22]. To our knowledge, this is the first study to develop and validate a non-invasive, peripheral blood circRNA-based nomogram for dynamic risk stratification in CML, integrating molecular biomarkers with routine hematological parameters to outperform conventional prognostic scores. Beyond diagnostic implications, the present study highlights the prognostic significance of hsa_circ_0001523 and hsa_circ_0000095 for CML survival outcomes. Patients exhibiting high hsa_circ_0001523 and low hsa_circ_0000095 expression had markedly shorter survival times. This correlation was robustly validated using univariate Cox regression analysis. These results are consistent with the mechanistic insights provided by Ji et al. [22], who implicated circRNAs in oncogenic signaling pathways that are frequently dysregulated in CML, such as Wnt/β-catenin. The ability of circRNAs to serve as both miRNA sponges and pathway modulators further enhances their utility as biomarkers [23-25]. For instance, hsa_circ_0001523 may promote leukemogenesis by sequestering tumor-suppressive miRNAs, whereas hsa_circ_0000095 may exert protective effects via analogous mechanisms. Future studies should explore these molecular interactions to elucidate their therapeutic implications.

Multivariate Cox regression analysis identified the basophil ratio, blast cell percentage, and hemoglobin levels as independent prognostic factors, corroborating their inclusion in established scoring systems such as Sokal, Hasford, and EUTOS [26]. The incorporation of the basophilic granulocyte count into the Hasford score underscores its prognostic significance in CML progression, a correlation substantiated by our data [6]. Similarly, the prognostic value of blast cells aligns with their well-documented role in disease acceleration. A decrease in hemoglobin levels was identified as an independent prognostic factor; lower values correlated with disease progression. Ko et al. [27] linked anemia to poor imatinib response, whereas Chen et al. [28] reported a rare case of CML arising from paroxysmal nocturnal hemoglobinuria. These studies suggest a plausible mechanistic interplay between erythropoietic dysfunction and leukemogenesis. However, the molecular underpinnings of the prognostic value of hemoglobin warrant further study. The HR for the basophil% category (0.01 - 0.04) exhibited an unexpected trend in the multivariate model. This may indicate complex interactions or multicollinearity among the included variables. How-

ever, larger independent cohorts are required to validate these results.

Our circRNA-based nomogram provides a non-invasive solution for CML management. It addresses unmet clinical needs through dynamic risk stratification based on peripheral blood analysis. The nomogram demonstrated superior DCA (AUC = 0.920) compared to traditional EUTOS (AUC = 0.76 - 0.82) and Sokal scores (AUC = 0.68 - 0.74) in our cohort [26], particularly for early progression prediction. The model established by Li et al. requires baseline bone marrow samples for BCR-ABL1 quantification. In contrast, our PB circRNA assay enables repeated testing with minimal patient burden; this is a critical advantage for long-term monitoring [29]. As highlighted by Rudich et al. [30] such models are particularly valuable for the early detection of progression in TKI-treated patients, where timely intervention is crucial. Clinicians can use the nomogram by inputting a patient's hsa_circ_0001523/hsa_circ_0000095 expression levels, basophil%, blast%, and hemoglobin levels. They can subsequently sum the scores to stratify patients into high- (score > 122.5) or low-risk (score ≤ 122.5) groups; high-risk patients may require more frequent monitoring (e.g., qRT-PCR every 3 months) or an early switch to second-generation TKIs.

This study has several notable strengths. It presents the first non-invasive, peripheral blood-based circRNA nomogram for dynamic risk stratification in chronic myeloid leukemia, eliminating the need for repeated bone marrow sampling. By integrating two phase-specific circRNAs with routine hematological parameters, the model achieves high discriminative accuracy (AUC = 0.920) - substantially outperforming conventional prognostic scores. Its reliance on qRT-PCR and standard blood tests, combined with validation in a large cohort of 417 patients, supports feasibility for near-term clinical translation.

Although our circRNA-based nomogram showed promising prognostic accuracy, this study had several limitations. First, the single-center retrospective design may limit generalizability to broader populations. Thus, external validation is required to confirm its clinical utility. Second, although bioinformatic analysis suggested miRNA sponge mechanisms for hsa_circ_0001523/0000095, direct experimental validation through functional studies is lacking. Third, the technical variability in circRNA quantification across laboratories and the performance of the model for rare CML variants require further evaluation. Fourth, the relatively small healthy control cohort (n = 45) may limit the robustness of between-group expression comparisons, though both circRNAs showed highly significant dysregulation ($p < 0.0001$, Figure 1). Future multicenter prospective studies with standardized protocols are required to address these limitations and facilitate clinical implementation.

In summary, this study demonstrates that hsa_circ_0001523 and hsa_circ_0000095 are significantly associated with CML progression. We constructed a nomogram model for predicting adverse outcomes in CML by detecting stable, abundant, and tissue-specific circRNAs in peripheral blood. The model is simple, practical, and easily applicable in clinical settings. Thus, it provides a noninvasive option for CML prognosis monitoring with broad clinical potential and value.

Acknowledgment:
The authors thank all the participants for donating blood samples and all the researchers for their contributions to this work.

Source of Funds:
This research was funded by the Basic Scientific Research Project of Wenzhou City (Y20220744).

Declaration of Generative AI in Scientific Writing:
Generative AI tools (e.g., "ChatGPT 4") were used only for polishing English grammar and style. All suggestions were critically reviewed and revised by the authors, who take full responsibility for the final content. No other AI tool was employed.

Declaration of Interest:
All authors declare no competing interests.

References:

1. Minciacchi VR, Kumar R, Krause DS. Chronic Myeloid Leukemia: A Model Disease of the Past, Present and Future. Cells 2021;10(1):117. (PMID: 33435150)

2. Jabbour E, Kantarjian H. Chronic myeloid leukemia: 2022 update on diagnosis, therapy, and monitoring. Am J Hematol 2022;97(9):1236-56. (PMID: 35751859)

3. Kantarjian HM, Hughes TP, Larson RA, et al. Long-term outcomes with frontline nilotinib versus imatinib in newly diagnosed chronic myeloid leukemia in chronic phase: ENESTnd 10-year analysis. Leukemia 2021;35(2):440-53. (PMID: 33414482)

4. Iezza M, Cortesi S, Ottaviani E, et al. Prognosis in Chronic Myeloid Leukemia: Baseline Factors, Dynamic Risk Assessment and Novel Insights. Cells 2023;12(13):1703. (PMID: 37443737)

5. Kaehler M, Cascorbi I. Molecular Mechanisms of Tyrosine Kinase Inhibitor Resistance in Chronic Myeloid Leukemia. Handb Exp Pharmacol 2023;280:65-83. (PMID: 36882601)

6. Hasford J, Baccarani M, Hoffmann V, et al. Predicting complete cytogenetic response and subsequent progression-free survival in 2060 patients with CML on imatinib treatment: the EUTOS score. Blood 2011;118(3):686-92. (PMID: 21536864)

7. Lauseker M, Hoffmann VS, Pfirrmann M. Prognostic scoring systems in chronic myeloid leukaemia. Leukemia 2025;39(5):1046-52. (PMID: 40234613)

8. Kristensen LS, Jakobsen T, Hager H, Kjems J. The emerging roles of circRNAs in cancer and oncology. Nat Rev Clin Oncol 2022;19(3):188-206. (PMID: 34912049)

9. He Z, Zhu Q. Circular RNAs: Emerging roles and new insights in human cancers. Biomed Pharmacother 2023;165:115217. (PMID: 37506578)

10. Zhao J, Wang G, Yan G, et al. Hsa_circ_0006010 and hsa_circ_0002903 in peripheral blood serve as novel diagnostic, surveillance and prognostic biomarkers for disease progression in chronic myeloid leukemia. BMC Cancer 2024;24(1):1172. (PMID: 39304860)

11. Pan Y, Lou J, Wang H, et al. CircBA9.3 supports the survival of leukaemic cells by up-regulating c-ABL1 or BCR-ABL1 protein levels. Blood Cells Mol Dis 2018;73:38-44. (PMID: 30224298)

12. Cao HX, Miao CF, Sang LN, et al. Circ_0009910 promotes imatinib resistance through ULK1-induced autophagy by sponging miR-34a-5p in chronic myeloid leukemia. Life Sci 2020;243:117255. (PMID: 31923418)

13. Can C, Yang X, Jia H, et al. Exosomal circ_0006896 promotes AML progression via interaction with HDAC1 and restriction of antitumor immunity. Mol Cancer 2025;24(1):4. (PMID: 39762891)

14. Balachandran VP, Gonen M, Smith JJ, DeMatteo RP. Nomograms in oncology: more than meets the eye. Lancet Oncol 2015;16(4):e173-80. (PMID: 25846097)

15. Baccarani M, Deininger MW, Rosti G, et al. European LeukemiaNet recommendations for the management of chronic myeloid leukemia: 2013. Blood 2013;122(6):872-84. (PMID: 23803709)

16. Hochhaus A, Baccarani M, Silver RT, et al. European LeukemiaNet 2020 recommendations for treating chronic myeloid leukemia. Leukemia 2020;34(4):966-84. (PMID: 32127639)

17. Memczak S, Jens M, Elefsinioti A, et al. Circular RNAs are a large class of animal RNAs with regulatory potency. Nature 2013;495(7441):333-8. (PMID: 23446348)

18. Glažar P, Papavasileiou P, Rajewsky N. circBase: a database for circular RNAs. RNA 2014;20(11):1666-70. (PMID: 25234927)

19. Livak KJ, Schmittgen TD. Analysis of relative gene expression data using real-time quantitative PCR and the 2(-Delta C(T)) Method. Methods 2001;25(4):402-8. (PMID: 11846609)

20. Zhang L, Bu Z, Shen J, Shang L, Chen Y, Wang Y. A novel circular RNA (hsa_circ_0000370) increases cell viability and inhibits apoptosis of FLT3-ITD-positive acute myeloid leukemia cells by regulating miR-1299 and S100A7A. Biomed Pharmacother 2020;122:109619. (PMID: 31919040)

21. Ye B, Qiao K, Zhao Q, Jiang Z, Hu N, Wang F. Tanshinone I restrains osteosarcoma progression by regulating circ_0000376/miR-432-5p/BCL2 axis. Mol Cell Biochem 2022;477(1):1-13. (PMID: 34532813)

22. Ji T, Chen Q, Tao S, et al. The research progress of circular RNAs in hematological malignancies. Hematology 2019;24(1):727-31. (PMID: 31581903)

23. Bi J, Pu Y, Yu X. Exosomal circ_0004136 enhances the progression of pediatric acute myeloid leukemia depending on the regulation of miR-570-3p/TSPAN3 axis. Anticancer Drugs 2021;32(8):802-11. (PMID: 33853086)

24. Wang Y, Wu C, Du Y, et al. Expanding uncapped translation and emerging function of circular RNA in carcinomas and noncarcinomas. Mol Cancer 2022;21(1):13. (PMID: 34996480)

25. Wu Y, Wei Y, Li Y, et al. Sperm-Derived CircRNA-1572 Regulates Embryogenesis and Zygotic Genome Activation by Targeting CCNB2 via Bta-miR-2478-L-2. Adv Sci (Weinh) 2025;12(18):e2414325. (PMID: 40091686)

26. Uz B, Buyukasik Y, Atay H, et al. EUTOS CML prognostic scoring system predicts ELN-based 'event-free survival' better than Euro/Hasford and Sokal systems in CML patients receiving frontline imatinib mesylate. Hematology. 2013;18(5):247-52. (PMID: 23540886)

27. Ko PS, Yu YB, Liu YC, et al. Moderate anemia at diagnosis is an independent prognostic marker of the EUTOS, Sokal, and Hasford scores for survival and treatment response in chronic-phase, chronic myeloid leukemia patients with frontline imatinib. Curr Med Res Opin 2017;33(10):1737-44. (PMID: 28715941)

28. Chen Y, Tao S, Deng Y, Song L, Yu L. Chronic myeloid leukemia transformation in a patient with paroxysmal nocturnal hemoglobinuria: a rare case report with literature review. Int J Clin Exp Med 2015;8(5):8226-9. (PMID: 26221399)

29. Li Y, Zhang Y, Wang J, et al. Development and validation of a nomogram to predict poor efficacy of imatinib in the treatment of newly diagnosed chronic phase chronic myeloid leukemia patients. Front Oncol 2024;14:1418417. (PMID: 38978732)

30. Rudich A, Garzon R, Dorrance A. Non-Coding RNAs Are Implicit in Chronic Myeloid Leukemia Therapy Resistance. Int J Mol Sci 2022;23(20):12271. (PMID: 36293127)

Additional material can be found online at:
http://supplementary.clin-lab-publications.com/251027/